InGaAs/AlGaAs intersubband transition structures grown on InAlAs buffer layers on GaAs substrates by molecular beam epitaxy

D. S. Katzer,[a] W. S. Rabinovich, and G. Beadie

U.S. Naval Research Laboratory, 4555 Overlook Avenue, S.W., Washington, D.C. 20375-5347

We report on the use of InAlAs linearly graded buffer layers for improving the performance of $In_yGa_{1-y}As$ ($y > 0.42$)/AlGaAs intersubband transition (ISBT) superlattice structures grown on GaAs substrates by molecular beam epitaxy. Linearly graded InAlAs buffer layers give better optical confinement in the active superlattice region, similar intersubband transition linewidths, and comparable surface morphology compared to linearly graded InGaAs buffer layers. The best surface morphology for our ISBT superlattices was obtained by growing the linearly graded InAlAs buffer layer at 360 °C. [S0734-211X(00)05103-9]

I. INTRODUCTION

Intersubband (ISB) transitions (ISBT) in superlattices have been used for mid-IR nonlinear optics and lasers using wide band gap materials for several years.[1–3] While GaAs/AlGaAs ISB structures have many advantages including ease of growth and lattice matching, they can only allow ISBT energies corresponding to wavelengths as short as 4 μm, but no shorter, due to the small conduction band offset. The most successful materials system for producing shorter wavelength transitions has been highly strained InGaAs/AlGaAs grown on a linearly graded InGaAs buffer layer. The strained $In_yGa_{1-y}As$/AlGaAs materials system requires the use of a strain-compensating buffer layer to grow thick, high quality superlattice structures when $y > 0.2$. Linearly graded buffers serve this function by acting as an artificial substrate with a lattice constant equal to the average lattice constant of the multiple quantum well (MQW) region.

Graded InGaAs buffer layers have been shown to be an effective way to grow high indium content InGaAs on GaAs substrates. In particular, Chui *et al.* showed that InGaAs/AlAs MQWs with ISBTs at wavelengths as short as 2 μm could be grown using a graded InGaAs buffer.[4] More recently, Sung *et al.* have demonstrated ISBTs at wavelengths around the 1.55 μm communications band using the same growth techniques.[5] However, the use of an InGaAs buffer layer limits the optical applications due to its refractive index properties. In the midinfrared, the index of refraction of $In_yGa_{1-y}As$ with $y < 0.50$ is between 3.35 and 3.45, while the index of refraction of AlAs is about 3.0. As a result, the index of the graded InGaAs buffer is often higher than the average index of the InGaAs/AlAs quantum wells. Thus, in a waveguide structure, the optical power is trapped in the buffer rather than in the quantum wells.

For the same indium mole fraction, InAlAs has a similar lattice constant as that of InGaAs but a lower refractive index. This makes it potentially appealing for buffer and cladding layer applications. Recently, the use of InAlAs buffers has been investigated. Bulk InGaAs layers grown on graded InAlAs buffers have been characterized by Wang *et al.*[6] and

Chyi *et al.*[7] and InGaAs electroabsorption waveguide modulators have been grown on step-graded InAlAs buffers by Loi *et al.*[8] These works have shown that good quality InGaAs layers can be grown on GaAs using a variety of InAlAs buffer structures. We extended these works by growing ISB MQWs on linearly graded InAlAs buffer layers.

In addition to their useful optical device properties, ISBTs in MQWs can also be used as a diagnostic probe of material quality. This is a result of the fact that the linewidths of ISBTs are more sensitive to interface quality than are the linewidths of excitons examined by photoluminescence.[9] The device requirements for operation in the midinfrared mean that the structures and buffers must often be thicker than comparable structures which operate at shorter wavelengths. This places constraints on the allowable strain in the structure. Finally, the presence of a waveguide structure in the material places constraints on the allowable surface roughness. Increased roughness will lead to higher waveguide losses and poorer device performance. In this article we investigate the effect of linearly graded InAlAs buffers on ISBTs in InGaAs/AlGaAs MQWs and compare the results to those obtained from structures grown by molecular beam epitaxy (MBE) on linearly graded InGaAs buffers.

II. EXPERIMENT

A. MBE system description

The ISB superlattice samples were grown in an early model Vacuum Generators V80H MBE system that uses conventional solid sources and also has a radio-frequency (rf) plasma source for the growth of GaN and related compounds. This system has eight effusion cell ports and is pumped by a 400 l/s ion pump, a titanium sublimation pump, and a 1500 l/s cryopump mounted on a high-conductance mitered elbow. The group III effusion cells were installed with two standard double-sided Conflat spacer flanges to move them back from the shutters by 1.36 in. to improve the flux uniformity[10,11] and to reduce shutter-induced flux transients.[12] In addition, the gallium and indium effusion cells used a ''tilted insert'' crucible to direct the flux toward the center of the wafer to improve the uniformity.[13] A coni-

---

Report Documentation Page

Form Approved
OMB No. 0704-0188

Public reporting burden for the collection of information is estimated to average 1 hour per response, including the time for reviewing instructions, searching existing data sources, gathering and maintaining the data needed, and completing and reviewing the collection of information. Send comments regarding this burden estimate or any other aspect of this collection of information, including suggestions for reducing this burden, to Washington Headquarters Services, Directorate for Information Operations and Reports, 1215 Jefferson Davis Highway, Suite 1204, Arlington VA 22202-4302. Respondents should be aware that notwithstanding any other provision of law, no person shall be subject to a penalty for failing to comply with a collection of information if it does not display a currently valid OMB control number.

1. REPORT DATE **2000**	2. REPORT TYPE	3. DATES COVERED **00-00-2000 to 00-00-2000**

4. TITLE AND SUBTITLE	5a. CONTRACT NUMBER
InGaAs/AIGaAs intersubband transition structures grown on InAIAs buffer layers on GaAs substrates by molecular beam epitaxy	5b. GRANT NUMBER
	5c. PROGRAM ELEMENT NUMBER
6. AUTHOR(S)	5d. PROJECT NUMBER
	5e. TASK NUMBER
	5f. WORK UNIT NUMBER

7. PERFORMING ORGANIZATION NAME(S) AND ADDRESS(ES) **Naval Research Laboratory,4555 Overlook Avenue, SW,Washington,DC,20375**	8. PERFORMING ORGANIZATION REPORT NUMBER

9. SPONSORING/MONITORING AGENCY NAME(S) AND ADDRESS(ES)	10. SPONSOR/MONITOR'S ACRONYM(S)
	11. SPONSOR/MONITOR'S REPORT NUMBER(S)

12. DISTRIBUTION/AVAILABILITY STATEMENT
Approved for public release; distribution unlimited

13. SUPPLEMENTARY NOTES

14. ABSTRACT

15. SUBJECT TERMS

16. SECURITY CLASSIFICATION OF:			17. LIMITATION OF ABSTRACT	18. NUMBER OF PAGES	19a. NAME OF RESPONSIBLE PERSON
a. REPORT **unclassified**	b. ABSTRACT **unclassified**	c. THIS PAGE **unclassified**		**5**	

Standard Form 298 (Rev. 8-98)
Prescribed by ANSI Std Z39-18

cal crucible effusion cell with a cold lip was used for the aluminum source. 8-nines (99.999999% pure) gallium, zone-refined 6-nines aluminum, 7-nines indium, 7-nines-5 arsenic, 6-nines beryllium, and a section of a high-resistivity float-zone-refined silicon wafer were used as the source materials. The arsenic beam equivalent pressure (BEP) was typically 15 times the total group III BEP during the InGaAs and InAlAs growths. The GaAs growth rate was typically 0.5 monolayers/s (ML/s) for these structures.

The substrate heater in the MBE system was a custom-made pyrolytic graphite heating element encased in pyrolytic boron nitride. This heating element was obtained for improved heater reliability for the growth of III-nitride compounds. The indium-free mounted substrate temperature was calibrated by observing the GaAs oxide desorption temperature with reflection high-energy electron diffraction (RHEED) and with optical pyrometry, with some additional measurements made using infrared transmission spectroscopy.[14,15] For temperatures below 400 °C (the lower temperature limit of the pyrometer), extrapolations to room temperature were used. The heater was operated with constant current without thermocouple feedback. Although we expect that the substrate temperature may have changed during the initial growth of smaller band gap materials on the GaAs substrate,[14,15] especially at low substrate temperatures, we did not intentionally compensate for this effect. ''MBE ready'' (001)±0.5° semi-insulating GaAs substrates were used without any additional cleaning steps. After the GaAs surface oxide was desorbed from the surface, a thin layer of GaAs was grown (typically 0.25 μm) at 580–600 °C before the substrate temperature was reduced to the desired growth temperature for the ISB superlattice structure.

B. MBE growth parameters

The initial stages of MBE layer growth were monitored with a 10 kV RHEED system. Due to the unavoidable flux nonuniformity across the sample and the difficulty in obtaining RHEED oscillations from the geometric center of a small test sample, we did not calibrate our growth rates using RHEED intensity oscillations. We instead relied on BEP measurements made using a nude ion gauge and postgrowth measurements of test samples to calibrate our growth rates. For example, a calibration plot of $\log_{10}$ GaAs growth rate versus $\log_{10}$ Ga BEP is nearly linear over a fairly large range (0.2–2.0 monolayers/s) with a correlation coefficient R >0.998. We were able to obtain good run-to-run reproducibility by comparing measured BEP values with *ex situ* measurements over approximately a decade of pressure range. This calibration curve does shift over time as the source material is depleted from the crucible.

Growth rates were calculated by comparing optical characteristics measured at room temperature in a Fourier transform infrared spectrometer (FTIR) to those modeled by a standard transfer matrix model which takes any strain in the layers into account.[9] The GaAs/AlGaAs calibration samples for these structures were typically two 6–8 period Bragg mirror structures. The InGaAs growth rates and composi-

tions were also extracted with this technique by growing and measuring test modulator structures. This method allows us to quickly measure our growth rates for several materials in a single sample. InAlAs growth rates were calculated from the known InAs and AlAs growth rates. The excellent agreement between the measured FTIR spectrum and the modeled spectrum, discussed below, gives us confidence in our technique.

For our work on linear graded buffer layers, we used a grading rate of 16% per μm. Early attempts at the use of $In_yGa_{1-y}As$ graded buffers used a final InAs mole fraction, y, equal to the average indium content of the wells. Later efforts showed that better results could be obtained by using a y value larger than the average indium content.[16] Several theoretical and experimental works have since shown that linearly graded buffers, even those that are many times thicker than the critical thickness,[12] have residual strain in the topmost layer.[17] As a result, the lattice constant of the top layer of the buffer is not equal to the unstrained value. The amount of residual strain depends upon the material and grading rate. We used measurements of residual strain by Wang *et al.*[6] to determine our y values. The buffers were grown at a substrate temperatures of 360, 400, or 480 °C. The MQWs were grown at 400 °C. Our $In_yAl_{1-y}As$ graded buffer layers used y values equal to the average indium content of the MQWs.

After growth, the samples were removed from the MBE system and cleaved into 5 mm×5 mm pieces. No further processing was performed.

C. Measurements

We measured the ISBTs of the samples in a FTIR at room temperature. The background FTIR scan was taken without a sample mounted in place. We were able to eliminate etaloning in the spectrum through careful orientation of the sample at Brewster's angle and by using a linear polarizer to illuminate the sample with *p*-polarized light. The high doping of the samples and the large number of periods in the superlattices ensured that the ISBT was strong and easily separable from the baseline signal. Atomic force microscopy (AFM) measurements were made in air using a Digital Instruments Dimension 3100 Nanoscope. The root-mean-square (rms) surface roughness of a 25 μm×25 μm area was calculated and is shown in Table I.

III. RESULTS

Although nearly three dozen ISB samples have been grown during the course of this work, we will only discuss a subset of these samples in this article in terms of their surface morphology and ISBT characteristics. The structures are described briefly in Table I, and AFM measurements of the rms surface roughness are listed along with their optical properties.

We will discuss five structures grown on linearly graded InAlAs buffers and one structure grown on linearly graded InGaAs buffers. ISBT and AFM surface roughness measurements were taken on all six of these samples. Note that no

TABLE I. InGaAs/AlGaAs intersubband multiple quantum well structures studied and their surface roughness as measured by atomic force microscopy. Also included in the table are the intersubband transition (ISBT) energies, integrated absorption strength (IAS), and the FWHM linewidth of the ISBT in meV.

Sample	Structure	Surface roughness (nm)	ISBT energy (meV)	IAS (abs meV)	FWHM linewidth (meV)
1447	100 Å 20% InGaAs $150\times$(10 ML 50% InGaAs/5 ML 45% AlGaAs/6 ML 50% InGaAs/9 ML AlAs/Si delta-doped 2×10^{12} cm^{-2}/9 ML AlAs) Drop substrate temperature to 400 °C 1.62 μm, 0%–26% graded InAlAs buffer at 16%/μm (001) SI GaAs substrate, 480 °C	11.38	⋯	⋯	⋯
1539	100 Å 16% InGaAs $150\times$(14 ML AlAs/Si delta-doped 7.5×10^{11} cm^{-2}/14 ML AlAs/21 ML 45% InGaAs) 1.31 μm, 0%–21% graded InGaAs buffer at 16%/μm (001) SI GaAs substrate, 400 °C	7.54	248	2.67	31
1540	100 Å 16% InGaAs $150\times$(14 ML AlAs/Si delta-doped 7.5×10^{11} cm^{-2}/14 ML AlAs/21 ML 45% InGaAs) Drop substrate temperature to 400 °C 1.31 μm, 0%–21% graded InAlAs buffer at 16%/μm (001) SI GaAs substrate, 480 °C	5.99	246	2.35	30
1541	100 Å 16% InGaAs $150\times$(14 ML AlAs/Si delta-doped 7.5×10^{11} cm^{-2}/14 ML AlAs/21 ML 45% InGaAs) 1.31 μm, 0%–21% graded InAlAs buffer at 16%/μm (001) SI GaAs substrate, 400 °C	5.46	245	2.54	30
1542	100 Å 16% InGaAs $150\times$(14 ML AlAs/Si delta-doped 7.5×10^{11} cm^{-2}/14 ML AlAs/21 ML 45% InGaAs) Raise substrate temperature to 400 °C 1.31 μm, 0%–21% graded InAlAs buffer at 16%/μm (001) SI GaAs substrate, 360 °C	3.96	247	2.25	29
1543	100 Å 17% InGaAs $40\times$(5 ML 45% InGaAs/13.5 ML 40% AlGaAs/Si delta-doped 2×10^{12} cm^{-2}/13.5 ML 40% AlGaAs/11 ML 45% InGaAs/25 ML AlAs) 1.06 μm, 0%–17% graded InAlAs at 16%/μm (001) SI GaAs substrate, 400 °C	2.30	⋯	⋯	⋯

doped electrical contact layers are used in these samples because our optical applications for these ISBT structures do not require electrical contact.

A. Square well structures

Sample No. 1539 had an In$_y$Ga$_{1-y}$As buffer that was linearly graded from $y=0$ to 0.20 at a grading rate of 16%/μm and was grown at 400 °C. The MQWs, also grown at 400 °C, consisted of 150 periods of the following: an undoped 6.1 nm In$_{0.42}$Ga$_{0.58}$As well followed by an 8.1 nm AlAs barrier delta doped with Si in the center to a sheet density of 1.5 $\times10^{12}$ cm^2. Samples Nos. 1540–1542 were the same MQW structure as sample No. 1539, but the buffer layers were linearly graded InAlAs and were grown at different temperatures to allow a comparison of the surface morphology and ISBTs as a function of the substrate temperature during growth of the linearly graded buffer layer.

These samples were designed to have an ISBT energy of 258 meV. The measured ISBT energies are within 5% of this value. The predicted integrated absorption strength (IAS) is

3.12 abs meV. The measured ISB IAS fractions are about 25% lower than this value and they vary by about 10% in the linearly graded InAlAs buffer layer samples.

Figure 1 shows the absorption spectrum of sample No. 1541 measured in the FTIR. The ISBT in sample No. 1541 occurs at 245 meV (4.97 μm) and has a full width at half maximum (FWHM) of 31 meV. The line shape shows an asymmetry typical of broadening due to nonparabolicity of the subbands. The relative linewidth of 13% is typical of what we have found for ISBTs in square InGaAs/AlAs MQWs. In particular, samples Nos. 1539–1542 all have essentially the same ISBT linewidth. Based on our previous work, we expect that a large fraction of the linewidth is due to inhomogeneous broadening, primarily well-width fluctuations.[9]

All of the samples were specular to the naked eye but exhibited varying degrees of cross-hatching under a Nomarski interference microscope. The AFM surface roughness measurements correlated with the Nomarski observations.
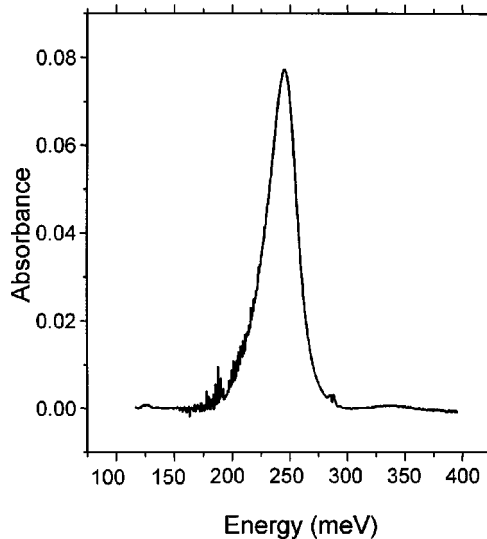
FIG. 1. Intersubband absorption spectrum measured on InGaAs/AlGaAs multiple quantum well sample No. 1541 grown on a linearly graded InAlAs buffer layer.

FIG. 2. Calculated lowest-order TE optical mode profiles for 3.74 μm wavelength radiation for a structure similar to InGaAs/AlGaAs multiple quantum well sample No. 1447 with an InAlAs buffer (solid line) and an InGaAs buffer (dashed line).

There may be several reasons for the differences in morphology between the samples. Sample No. 1543, which has the lowest roughness, is considerably thinner than the other samples. If our estimate of residual strain in the buffer was incorrect in the design of the structure, or if there were errors in the growth, thicker samples would be more likely to partially relax than thinner samples. As shown in Table I, a comparison of samples Nos. 1540–1542 reveals that the growth temperature of the buffer also plays a role.[18] In particular, we see that the surface roughness decreases from about 6 to about 4 nm as we decrease the growth temperature of the linearly graded InAlAs buffer layer from 480 to 360 °C. Thus the optimum growth temperature seems to be 360 °C for these structures, though in fact it may be lower as we have not yet seen an increase in roughness for linearly graded InAlAs buffer layers grown at lower temperatures.

We have seen little evidence that the low growth temperatures used for the buffer layers (480 to 360 °C) has affected the sheet carrier concentration in the MQW, as seen by the small variation in IAS shown in Table I. In general, we have found that doping in the barriers leads to higher sheet concentrations than doping in the wells. We believe this is because the energy of the carriers in the $n = 1$ state of the well is much lower than the conduction band of the barriers. This effect also tends to make these samples less susceptible to traps in the barriers. Additional optimization studies will be necessary to improve the surface morphology further.

B. Coupled well structures

Most devices that use ISBTs require more complicated structures than square wells of the type used in samples Nos. 1539–1542. To examine the effects of InAlAs buffers on such structures, we grew MQWs with a pair of InGaAs wells coupled through an intermediate AlGaAs barrier (samples Nos. 1447 and 1543). We have used similar structures in the
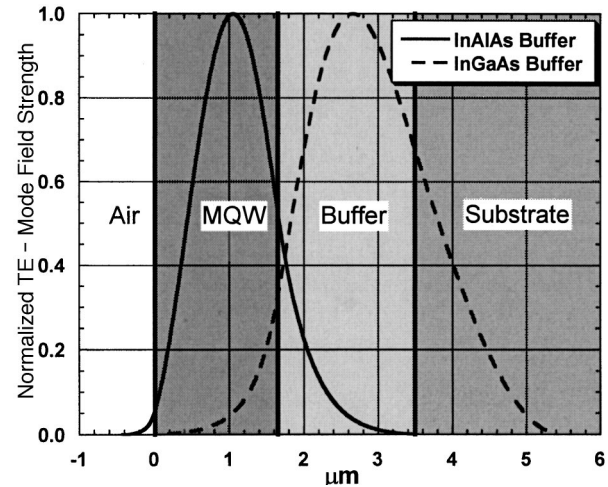
past to engineer ISBT materials with high values of n_2 (the nonlinear index of refraction).[19] In this study, sample No. 1543 was designed for nonlinear optical switching applications. It uses a coupled-well structure similar to that described in Ref. 19. In that case, the sample was grown on a linearly graded InGaAs buffer layer which could not act as a waveguide. Sample No. 1543 instead incorporates a linearly graded InAlAs single-mode optical waveguide layer designed for 1.55 μm light. Its absorption spectra is similar to that described in Ref. 19. The absorption spectra consists of a main peak at 3.55 μm corresponding to the levels 1–4 intersubband transition. Weaker peaks corresponding to the levels 1–3 and levels 2–3 ISBTs are found at 4.4 and 7.05 μm, respectively.

C. Waveguide structure

Sample No. 1447 is a coupled-well MQW structure which, like No. 1543, is also designed to act as a slab waveguide for midinfrared light. In Fig. 2 we show the lowest-order TE mode profile calculated for a MQW/waveguide structure using a transfer matrix method.[20] The calculation was based on the structure of sample No. 1447, with the only difference being the composition of the buffer. The calculation was made for a radiation wavelength of 3.74 μm, which is close to an ISBT resonance. In the calculation, we assumed that the index of refraction of the MQW was equal to the average index of the layers. The linear grade of the index in the buffer was explicitly included.

Because the InGaAs buffer has a higher average index of refraction than either the MQW or the substrate regions, the guided mode is clearly peaked in the buffer. Conversely, in the structure grown on the InAlAs buffer, the mode profile is centered in the MQW region. We find that over 90% of the optical power is contained within the MQW region for the InAlAs buffer structure, but less than 2% is contained within the MQW for the InGaAs buffer case. It is precisely for this reason that InAlAs buffers are of interest for the develop-

ment of optical devices based on the InGaAs/AlGaAs materials system.

It is important to note that discrepancies between the calculated and actual refractive indices exist, but they do not affect the conclusions we have drawn from the model. In particular, an effort was made to include the effects of the ISB resonance on the index of refraction via the Kramers–Kronig relationship. When included, however, this correction had a negligible impact on the mode confinement factors.

IV. CONCLUSIONS

We have grown MQWs of InGaAs/AlGaAs on both linearly graded InGaAs and linearly graded InAlAs buffers on GaAs substrates using MBE. Through careful modeling of the device structure and optimized growth conditions, we are able to obtain excellent agreement (within 5%) between the predicted and the measured ISBTs. The quality of the ISB resonances are similar for both types of buffers. The linearly graded InAlAs buffer, however, allows the fabrication of waveguide devices with much better mode confinement due to its lower index of refraction. While the ISBTs were not strongly affected by the buffer layer growth temperature, there were differences in the surface morphology of the samples. We find that with our growth conditions, for a 45% InGaAs/AlAs superlattice ISB structure, the best results are obtained by growing the linearly graded 21% InAlAs buffer layer at 360 °C. In addition to their useful optical properties, these ISB structures can be used as a MBE diagnostic tool since the ISBT wavelength is more sensitive to interface quality than is the superlattice PL linewidth.

ACKNOWLEDGMENTS

[1]B. F. Levine, K. K. Choi, C. G. Bethea, J. Walker, and R. J. Malik, Appl. Phys. Lett. **50**, 1092 (1987).
[2]J. Faist, F. Capasso, D. L. Sivco, A. L. Hutchinson, C. Sirtori, and A. Y. Cho, Science **264**, 553 (1994).
[3]J. B. Khurgin, *Second Order Intersubband Nonlinear Optical Susceptibilities of Asymmetric Quantum Well Structures* (Optical Society of America, Washington, D.C., 1989), pp. 1–69.
[4]H. C. Chui, G. L. Woods, M. M. Fejer, E. L. Martinet, and J. S. Harris, Jr., Appl. Phys. Lett. **66**, 265 (1995).
[5]B. Sung, H. C. Chui, M. M. Fejer, and J. S. Harris, Jr., Electron. Lett. **33**, 818 (1997).
[6]S. M. Wang, C. Larlson, N. Rorsman, M. Bergh, E. Olsson, T. G. Andersson, and H. Zirath, J. Cryst. Growth **175/176**, 1016 (1997).
[7]J.-I. Chyi, J.-L. Shieh, J.-W. Pan, and R.-M. Lin, J. Appl. Phys. **79**, 8367 (1996).
[8]K. K. Loi, L. Shen, H. H. Wieder, and W. S. C. Chang, IEEE Photonics Technol. Lett. **9**, 1229 (1996).
[9]G. Beadie, W. S. Rabinovich, D. S. Katzer, and M. Goldenberg, Phys. Rev. B **55**, 9731 (1996).
[10]Z. R. Wasilewski, G. C. Aers, A. J. SpringThorpe, and C. J. Miner, J. Cryst. Growth **111**, 70 (1991).
[11]G. C. Aers and Z. R. Wasilewski, J. Vac. Sci. Technol. B **10**, 815 (1992).
[12]F. G. Celii, Y. C. Kao, E. A. Beam III, W. M. Duncan, and T. S. Moise, J. Vac. Sci. Technol. B **11**, 1018 (1993).
[13]A. J. SpringThorpe, A. Majeed, C. J. Miner, Z. R. Wasilewski, and G. C. Aers, J. Vac. Sci. Technol. A **9**, 3175 (1991).
[14]B. V. Shanabrook, R. J. Waterman, J. L. Davis, R. J. Wagner, and D. S. Katzer, J. Vac. Sci. Technol. B **11**, 994 (1993).
[15]D. S. Katzer and B. V. Shanabrook, J. Vac. Sci. Technol. B **11**, 1003 (1993).
[16]H. C. Chui and J. S. Harris, Jr., J. Vac. Sci. Technol. B **12**, 1019 (1994).
[17]A. Sacedon, F. Gonzalez-Sanz, E. Calleja, E. Munoz, S. I. Molina, F. J. Pacheco, D. Araujo, R. Garcia, M. Lourenco, Z. Yang, P. Kidd, and D. Dunstan, Appl. Phys. Lett. **66**, 3334 (1995).
[18]L. Shen, H. H. Wieder, and W. S. C. Chang, IEEE Photonics Technol. Lett. **8**, 352 (1996).
[19]W. S. Rabinovich, G. Beadie, and D. S. Katzer, IEEE J. Quantum Electron. **34**, 975 (1998).
[20]D. Rafizadeh and S. T. Ho, Opt. Commun. **141**, 17 (1997); J. F. Offersgaard, J. Opt. Soc. Am. B **12**, 2122 (1995).